Luminescent Polycrystalline Cadmium Selenide Nanowires Synthesized by Cyclic Electrodeposition/Stripping Coupled with Step Edge Decoration

Q. Li, M. A. Brown, J. C. Hemminger, and R. M. Penner*

Department of Chemistry and Institute For Surface and Interface Science (ISIS), University of California, Irvine, California 92697-2025

Received February 2, 2006. Revised Manuscript Received April 17, 2006

Cadmium selenide (CdSe) nanowires, 30−300 nm in diameter, were synthesized using electrochemical step edge decoration on highly oriented pyrolytic graphite (HOPG) surfaces. These CdSe nanowires were more than 100 μm in length and were organized into parallel arrays of hundreds following the length and organization of the HOPG step edges used to nucleate these nanowires. The synthesis of CdSe nanowires involved a method derived from the cyclic electrodeposition/stripping scheme described by Sailor and co-workers (*Chem. Mater.* **1991**, *3*, 1015). Stoichiometric CdSe was obtained by electrodepositing CdSe together with excess elemental cadmium and selenium, followed by the selective oxidative stripping of both excess cadmium and selenium from these nanowires. This synthesis method also afforded precise control of the nanowire diameter over the above-mentioned range. CdSe nanowires were characterized by scanning electron microscopy, transmission electron microscopy (TEM), selected area electron diffraction, photoluminescence, X-ray photoelectron spectroscopy, and Raman spectroscopy. The TEM results showed that the CdSe nanowires were composed of nanocrystalline, cubic CdSe with a crystallite size that decreased with increasing pH. CdSe nanowires showed band edge photoluminescence at 1.74 eV that increased in intensity by a factor of 15 when these wires were covered by a shell of CdS by exposure to gaseous H_2S at 300 °C.

I. Introduction

Most everything now known about semiconductor nanowires has been derived from investigations of single crystalline materials. In the specific case of cadmium selenide, the material on which we focus here, work in this direction dates from 1999 with the first synthesis by Wang et al.[1] of CdSe nanorods by a solvothermal method. These nanowires were 8−20 nm in diameter and 150−500 nm in length. A year later, Alivasatos and co-workers[2] described the synthesis of CdSe nanorods with dimensions of 3−4 nm in diameter by 4−6 nm in length. Refinements to this synthesis by Peng and Peng[3] in 2001 yielded CdSe nanorods up to 25 nm in length with diameters still in the 2−5 nm range. Buhro and co-workers[4] investigated the diameter-dependent photoluminescence (PL) of CdSe nanowires synthesized using the solution−liquid−solid[5,6] method in 2003, demonstrating the transition from two-dimensional to three-dimensional exciton confinement as the diameter of the nanorods was reduced from 19 to 5 nm. Very recently, electronic transport within dendritic CdTe "tetrapods", synthesized in 2003 by Alivisatos and co-workers,[7] has been investigated by making electrical contacts to three of the four single crystalline arms of these structures.[8] Despite the intrinsic difficulty of manipulating and positioning individual crystallites from suspensions of these materials, a variety of optical and electronic devices exploiting CdSe nanocrystals have been demonstrated at a proof-of-concept level, for example, refs 9−15.

Polycrystalline semiconductor nanowires have not been as intensively studied, nor has it been possible, as far as we know, to synthesize polycrystalline CdSe nanowires with diameters small enough to exhibit any degree of quantum confinement. Most of the prior work in this direction has involved the electrodeposition of semiconductors within the pores of templates, especially porous alumina. Sailor and co-workers[16] were the first to demonstrate this concept in

* To whom correspondence should be addressed. E-mail: rmpenner@uci.edu.

(1) Wang, W. Z.; Geng, Y.; Yan, P.; Liu, F. Y.; Xie, Y.; Qian, Y. T. *Inorg. Chem. Commun.* **1999**, *2*, 83.
(2) Peng, X. G.; Manna, L.; Yang, W. D.; Wickham, J.; Scher, E.; Kadavanich, A.; Alivisatos, A. P. *Nature* **2000**, *404*, 59.
(3) Peng, Z. A.; Peng, X. G. *J. Am. Chem. Soc.* **2001**, *123*, 1389.
(4) Yu, H.; Li, J. B.; Loomis, R. A.; Gibbons, P. C.; Wang, L. W.; Buhro, W. E. *J. Am. Chem. Soc.* **2003**, *125*, 16168.
(5) Trentler, T. J.; Goel, S. C.; Hickman, K. M.; Viano, A. M.; Chiang, M. Y.; Beatty, A. M.; Gibbons, P. C.; Buhro, W. E. *J. Am. Chem. Soc.* **1997**, *119*, 2172.
(6) Trentler, T. J.; Hickman, K. M.; Goel, S. C.; Viano, A. M.; Gibbons, P. C.; Buhro, W. E. *Science* **1995**, *270*, 1791.
(7) Manna, L.; Milliron, D. J.; Meisel, A.; Scher, E. C.; Alivisatos, A. P. *Nat. Mater.* **2003**, *2*, 382.
(8) Cui, Y.; Banin, U.; Bjork, M. T.; Alivisatos, A. P. *Nano Lett.* **2005**, *5*, 1519.
(9) Chan, Y.; Caruge, J. M.; Snee, P. T.; Bawendi, M. G. *Appl. Phys. Lett.* **2004**, *85*, 2460.
(10) Chan, Y.; Steckel, J. S.; Snee, P. T.; Caruge, J. M.; Hodgkiss, J. M.; Nocera, D. G.; Bawendi, M. G. *Appl. Phys. Lett.* **2005**, *86*.
(11) Colvin, V. L.; Schlamp, M. C.; Alivisatos, A. P. *Nature* **1994**, *370*, 354.
(12) Huynh, W. U.; Dittmer, J. J.; Alivisatos, A. P. *Science* **2002**, *295*, 2425.
(13) Oertel, D. C.; Bawendi, M. G.; Arango, A. C.; Bulovic, V. *Appl. Phys. Lett.* **2005**, *87*.
(14) Schlamp, M. C.; Peng, X. G.; Alivisatos, A. P. *J. Appl. Phys.* **1997**, *82*, 5837.
(15) Sun, B. Q.; Marx, E.; Greenham, N. C. *Nano Lett.* **2003**, *3*, 961.

10.1021/cm060262l CCC: $33.50
Published on Web 06/22/2006

1993 with the fabrication by electrodeposition of arrays of diodes in which a CdSe segment was electrochemically grafted onto a gold segment. These CdSe/gold nanowires showed rectification, qualitatively as expected for Schottky barriers. Mallouk and co-workers[17] used a similar approach to synthesize ensembles of gold/CdSe/gold nanowires that showed photoconductivity. The advantage of template synthesis, exploited in both of these examples, is the relative ease with which compositionally segmented nanowires can be prepared. The maximum nanowire length, however, is bounded by the maximum template thickness which is typically 20−30 μm for alumina.

In this paper we describe a method for preparing arrays of hundreds of polycrystalline CdSe nanowires and CdSe-CdS core-shell nanowires that are 30−300 nm in diameter and more than 100 μm in length. This method, a variant of the electrochemical step edge decoration (ESED)[18−20] method developed in our lab, involves the electrodeposition of CdSe selectively at the step edges present on a highly oriented pyrolytic graphite (HOPG) surface. To achieve the growth of CdSe nanowires, ESED was coupled with a cyclic deposition/stripping regime in which CdSe and excess elemental selenium and cadmium were first electrodeposited onto HOPG by scanning the potential from the rest potential to −1 V versus the saturated calomel electrode (SCE); the potential was then scanned positively to +1 V to strip away both elemental Cd and Se, leaving near-stoichiometric CdSe nanowires on the graphite surface. This cyclic electrodeposition/stripping strategy was inspired by, and derived from, a method described by Sailor and co-workers.[21] It differs from the Sailor method in the use of a more positive stripping potential, necessary for the removal of excessive elemental selenium. As shown in Scheme 1, the localization of CdSe growth at step edges is facilitated by the preceding electrodeposition of selenium nuclei at step edges. These Se nuclei form with a very high linear nucleation density of $>30\ \mu m^{-1}$, thereby enabling the growth of extremely small CdSe nanowires with diameters in the 30 nm range. The deposition of CdSe nanowires is size-selective: the diameter of the CdSe nanowires can be controlled by varying the number of electrodeposition/stripping cycles. CdSe nanowires obtained using this procedure can be covered with a thin layer of CdS by exposure to H_2S at 300 °C (Scheme 1). This treatment, involving the substitution of selenium with sulfur at the surface of the nanowire, increases the intensity of emitted PL by a factor of 15, an effect that mimics the increased quantum yield for PL reported earlier for ZnS- and CdS-capped CdSe nanocrystals.[22,23] In this paper, we describe the synthesis, structural characterization, and optical properties of the CdSe and CdSe-CdS core-shell nanowires we have prepared. The initial goal of these investigations is to learn the degree to which the spectroscopic properties of polycrystalline CdSe nanowires resemble those of single crystalline CdSe nanorods.

Scheme 1

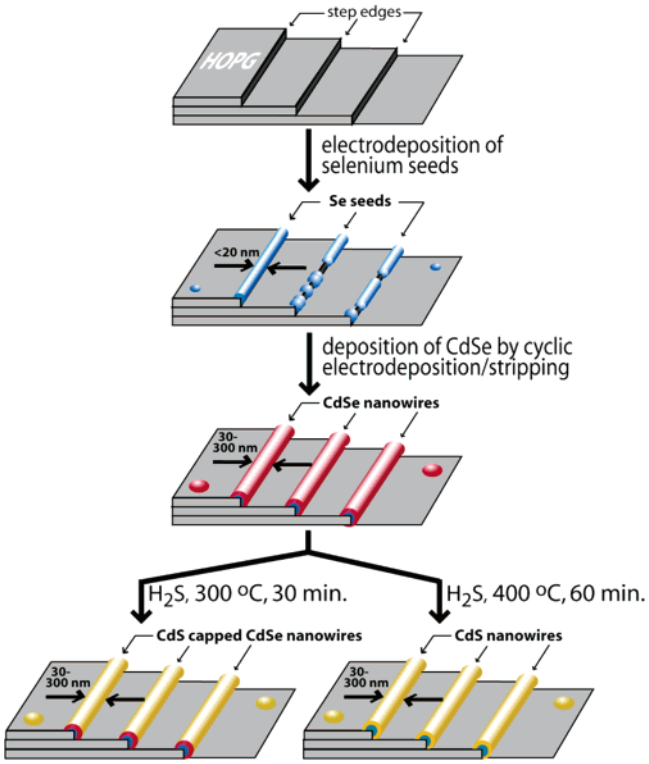

II. Experimental Section

Electrodeposition. Cadmium selenide nanowires were electrodeposited from aqueous plating solutions containing 80−120 mM $CdSO_4$ (Sigma-Aldrich, 99.99%) and 0.5−2 mM SeO_2 (Fisher, 99.99%) adjusted to pH 2.5−3.5 by adding sulfuric acid. These solutions were purged with N_2 for 30 min prior to each experiment. *Caution:* Both Cd^{2+} and SeO_2^{2-} are highly toxic, and extreme care must be exercised in the handling of aqueous solutions of these ions. These solutions were prepared using Barnsted nanopure water (ρ > 17 MΩ·cm). A basal plane oriented, 12 × 12 × 1 mm piece of HOPG was employed as the working electrode in a three-electrode cell with a large area platinum counter electrode and a reference SCE. The HOPG electrode was held in a Teflon holder in which a rubber O-ring isolated a 3.3 mm diameter area of the HOPG basal plane for exposure to the plating solution. Cyclic voltammetry was performed using a computer-controlled EG&G 2263 potentiostat by scanning the potential between +1 and −1 V versus SCE.

Electron Microscopy. Scanning electron microscopy (SEM) was carried out on uncoated or gold-coated samples using a Philips FEG-30XL microscope equipped with energy-dispersive X-ray (EDX) analysis elemental analysis capabilities. An accelerating voltage of 10 kV was used for SEM imaging, whereas for EDX analysis, 20 kV was used. Transmission electron microscopy (TEM) was carried using a Philips CM-20 with an accelerating voltage of 200 kV. HOPG flakes with attached nanowires were transferred to uncoated copper grids (uncoated copper, Ted Pella) for analysis using TEM. These flakes were obtained by peeling off a small piece of graphite covered with nanowires using Scotch tape.

(16) Klein, J. D.; Herrick, R. D.; Palmer, D.; Sailor, M. J.; Brumlik, C. J.; Martin, C. R. *Chem. Mater.* **1993**, *5*, 902.
(17) Pena, D. J.; Mbindyo, J. K. N.; Carado, A. J.; Mallouk, T. E.; Keating, C. D.; Razavi, B.; Mayer, T. S. *J. Phys. Chem. B* **2002**, *106*, 7458.
(18) Li, Q. G.; Olson, J. B.; Penner, R. M. *Chem. Mater.* **2004**, *16*, 3402.
(19) Walter, E. C.; Murray, B. J.; Favier, F.; Kaltenpoth, G.; Grunze, M.; Penner, R. M. *J. Phys. Chem. B* **2002**, *106*, 11407.
(20) Zach, M. P.; Ng, K. H.; Penner, R. M. *Science* **2000**, *290*, 2120.
(21) Kressin, A. M.; Doan, V. V.; Klein, J. D.; Sailor, M. J. *Chem. Mater.* **1991**, *3*, 1015.
(22) Peng, X. G.; Schlamp, M. C.; Kadavanich, A. V.; Alivisatos, A. P. *J. Am. Chem. Soc.* **1997**, *119*, 7019.
(23) Manna, L.; Scher, E. C.; Li, L. S.; Alivisatos, A. P. *J. Am. Chem. Soc.* **2002**, *124*, 7136.

Photoluminescence. Luminescence spectra were acquired using 50 mW continuous wave excitation from a Lexel Model 95-SHG intracavity double argon ion laser at 257 nm. Power densities of ~150 W cm^{-2} at the sample were typical. Laser light with p polarization was incident on the sample at Brewster's angle (~60°) from the surface normal. Emission was collected at normal incidence through a 20× Zeiss EpiPlan microscope objective, NA 0.45. The light was then coupled with an f4 lens into an imaging spectrograph (Chromex 250IS, equipped with 1200 and 300 grooves mm^{-1} holographic gratings, both 500 nm blaze) which dispersed the light onto a liquid nitrogen cooled charge-coupled device (CCD; Princeton Instruments model LN/1024EUV) having 1024 × 256 pixels. Signals from the 256 pixels arrayed perpendicular to the long axis of the CCD were binned, producing a linear detector with 1024 channels. The pixel-wise resolution of this detector was 0.6 and 2.3 meV using the 1200 and 300 grooves mm^{-1} gratings, respectively. Collection times varied between 1 and 30 s.

X-ray Photoelectron Spectroscopy (XPS). XPS measurements were performed with an ESCALAB MKII (VG Scientific) surface analysis system. The system is a multichamber ultrahigh vacuum system equipped with a twin anode X-ray source (Mg/Al) and a 150 mm hemispherical electron energy analyzer. Spectra presented here were obtained using Mg Kα X-rays (1253.6 eV). During these experiments the base pressure in the spectroscopy chamber was 1 × 10^{-9} Torr. The experiments were carried out with the energy analyzer in constant analyzer energy mode and at a pass energy of 20 eV. The peak positions were calibrated using the C(1s) peak of the HOPG substrate at 284.5 eV as a reference.[24]

III. Results and Discussion.

III.A. CdSe Nanowire Nucleation. CdSe nanowires were prepared by ESED, the selective electrodeposition of CdSe at step edges on the freshly cleaved HOPG surface. Previously, ESED has been used to prepare noble metal nanowires,[19] metal oxide nanowires,[18,20] metal sulfide nanowires,[25,26] and Bi_2Te_3[27] nanowires. Nanowires are obtained when nuclei of the deposited material are formed preferentially and at a high linear density (δ, units of μm^{-1}), on step edge defects. In fact, for hemispherical nuclei simple geometrical arguments require that $\delta > 1/d$, where d is the nanowire diameter. In the previous studies cited above, we found that nucleation typically occurred with δ values of ≈ 10 μm^{-1} after optimization of the nanowire growth conditions. Thus, the smallest wires obtainable from these nuclei were approximately 100 nm in diameter.

For the growth of CdSe nanowires described here, we obtained significantly higher δ values, up to 30 μm^{-1}. But this unusually high nucleation density was only observed when the supporting electrolyte was excluded from the deposition solution, as demonstrated by data shown in Figure 1. Cyclic voltammograms (CVs) for a HOPG electrode in aqueous solutions containing 100 mM $CdSO_4$ and 0.5 mM SeO_2 with and without 0.50 M Na_2SO_4 (Figure 1a) both show

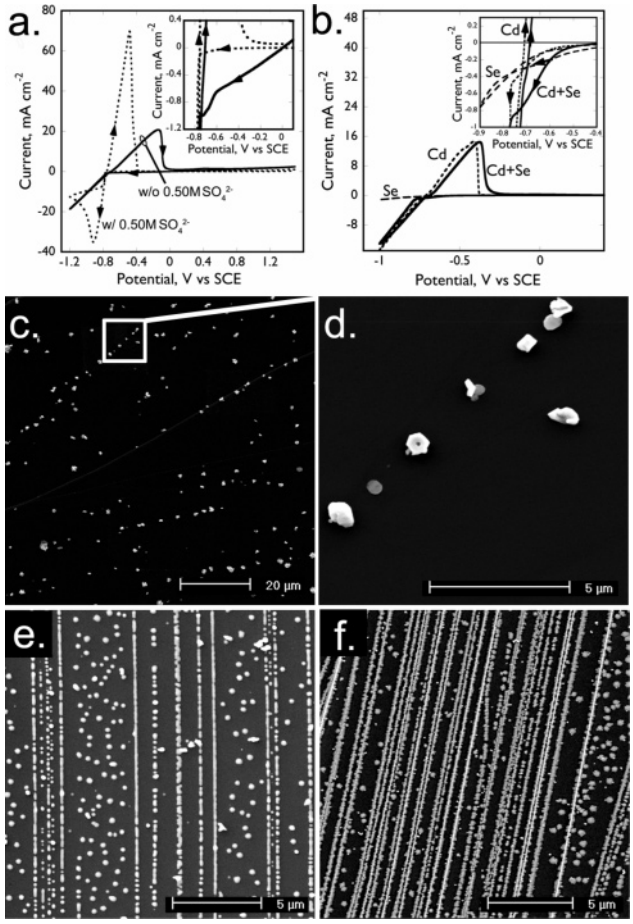

Figure 1. (a) Effect of supporting electrolyte on plating CVs: CVs at 20 mV s^{-1} for the HOPG basal plane in a plating solution containing aqueous 100 mM $CdSO_4$ and 0.5 mM SeO_2 with 0.5 M Na_2SO_4 (dashed lines) and without added Na_2SO_4 (solid lines). Inset: magnified view of the potential region between −0.9 and 0.1 V vs SCE. (b) Identification of −0.6 to −0.8 V "prewave". Three CVs are shown for three different plating solutions: (Se) 2 mM SeO_2, dashed line; (Cd) 80 mM $CdSO_4$, dotted line; and (Cd+Se) 80 mM $CdSO_4$ and 0.8 mM SeO_2, solid line. (c−f) SEM images of a HOPG surface after a linear scan voltammogram from the rest potential to −0.9 V at 20 mV s^{-1} in (c, d) 80 mM $CdSO_4$, (e) 2 mM SeO_2, and (c) 80 mM $CdSO_4$ and 0.80 mM SeO_2.

a reduction wave and an oxidation wave that is coupled to it. The flattening of these voltammetric waves, in the case of the solution without supporting electrolyte, is expected on the basis of the high ohmic resistance of this solution. A closer inspection of the potential interval from −0.4 V versus SCE and −0.8 V (Figure 1a, inset) shows a second, unexpected effect: in the Na_2SO_4-free solution, the onset for cathodic current is near −0.10 V and the onset for a second faradic process is seen at −0.62 V. We found empirically that the cathodic processes that occur within this range from −0.10 V to −0.65 V in the absence of Na_2SO_4 enable the synthesis of CdSe nanowires. In the presence of 0.5 M Na_2SO_4, nanowires of CdSe could not be obtained because the number of CdSe nuclei that formed along step edges was far too sparse ($\delta < 5$ μm^{-1}; data not shown). This observation suggests that reduction processes occurring in the range from −0.10 V to −0.65 V are involved in the nucleation of CdSe nuclei along HOPG step edges, but what are these reduction processes?

To answer this question, two experiments were carried out. First, the potential of HOPG electrodes was scanned at 20

(24) Moulder, J. F.; Stickle, W. F.; Sobol, P. E.; Bomben, K. D. *Handbook of X-ray Photoelectron Spectroscopy*; Perkin-Elmer Corp., Physical Electronics Division: Eden Prarie, MN, 1992.
(25) Li, Q.; Newberg, J. T.; Walter, E. C.; Hemminger, J. C.; Penner, R. M. *Nano Lett.* **2004**, *4*, 277.
(26) Li, Q.; Walter, E. C.; van der Veer, W. E.; Murray, B. J.; Newberg, J. T.; Bohannan, E. W.; Switzer, J. A.; Hemminger, J. C.; Penner, R. M. *J. Phys. Chem. B* **2005**, *109*, 3169.
(27) Menke, E. J.; Li, Q.; Penner, R. M. *Nano Lett.* **2004**, *4*, 2009.

mV s^{-1} from the rest potential of the HOPG surface to −0.90 V in plating solutions containing each of the two nanowire constituents: Cd^{2+} and Se (as H_2SeO_3), as well as a solution containing both Cd and Se. SEM and EDX elemental analysis were used to characterize the resulting electrode surfaces. In this experiment, the final electrode potential was −0.9 V, and nothing was subsequently stripped from the electrodeposit. In the solution containing only $CdSO_4$, the reduction to cadmium metal occurred with a sharp onset at −0.76 V (Figure 1b):

$$Cd \rightarrow Cd^{2+} + 2e^- \quad (1)$$

This is a reversible process, and a cadmium oxidation wave is observed on the reverse scan at −0.71 V, just positive of the plating onset. The reversibility of this process at HOPG is typical of what we have observed previously for coinage metals such as Ag, Cu, Ni, and so forth.[20,26] In general, we have found that the high kinetic facility of these reactions correlates with a low nucleation density for these metals on HOPG step edges, often in the 1 μm^{-1} range. As the SEM images of Figure 1c,d clearly show, this is exactly what we observe for cadmium: Cadmium nanocrystallites are produced at step edges, but these particles are formed with δ = 0.2−1.0 μm^{-1}. In a solution containing Se only, in contrast, the CV is highly irreversible with a gradual onset near −0.38 V and no oxidation peak on the reverse scan (Figure 1b). Previously this reduction has been assigned as a six-electron reduction of H_2SeO_3 to H_2Se:[28]

$$H_2SeO_3 + 6H^+ + 6e^- \rightarrow H_2Se + 3H_2O \quad (2)$$

However, H_2Se is oxidized to elemental Se at −0.740 V versus SCE under the conditions of pH and SeO_2 concentration that apply here:[29]

$$H_2Se \rightarrow Se + 2H^+ + 2e^- \quad (3)$$

The material actually observed in the SEM of Figure 1e is either SeO_2 or SeO_2-passivated selenium metal because these surfaces experience approximately 1 h of air exposure prior to SEM imaging. The SEM of this HOPG surface (Figure 1e) shows a much higher nucleation density than was seen for cadmium and even the production of some continuous nanowires. A similar result was seen when this experiment was repeated for a solution containing both cadmium and selenium (Figure 1f). The CV for this "Cd + Se" solution shows a gradual onset for reduction near −0.60 V that quickly produces more reduction current than seen in the Se-only experiment. This CdSe deposition current is augmented by a second, faster cadmium reduction at −0.78 V followed by cadmium stripping at −0.70 V if the scan is reversed. We presume that the CdSe obtained in this experiment is produced by a direct $6e^-$ reduction as proposed by Mishra and Rajeshwar:[30]

$$H_2SeO_3 + Cd^{2+} + 6e + 4H^+ \rightarrow CdSe + 3H_2O \quad (4)$$

The main conclusion of this series of experiments is that

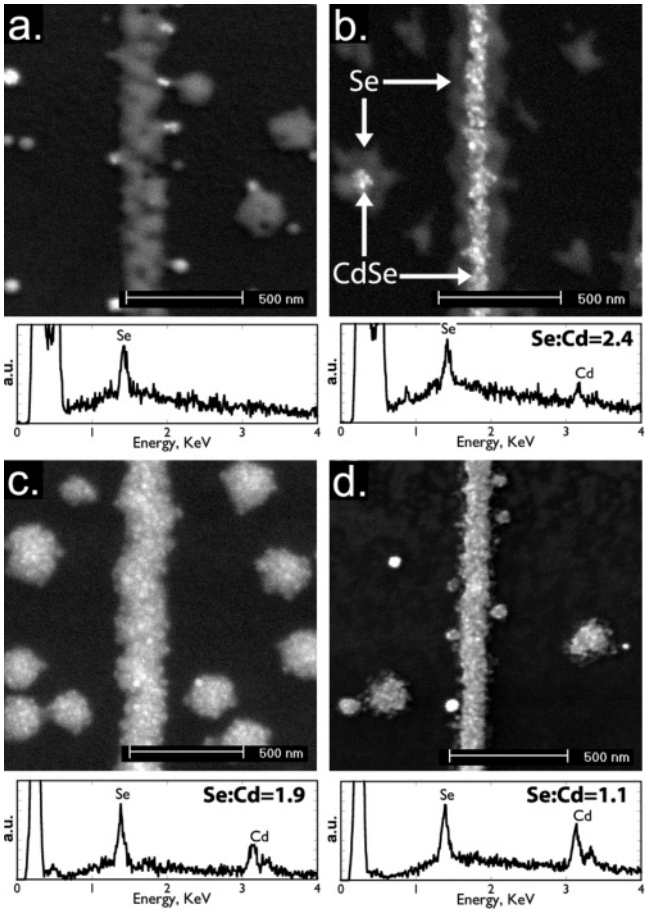

Figure 2. SEM images of HOPG electrode after scanning the potential between 0.6 V and different negative limits, $E_{(-)}$, at 20 mV s^{-1} for three cycles: (a) $E_{(-)}$ = −0.60 V vs SCE, (b) $E_{(-)}$ = −0.80 V, (c) $E_{(-)}$ = −1.0 V, and (d) $E_{(-)}$ = −0.8 V followed by annealing in N_2 at 300 °C for 30 min. The Se:Cd atomic ratios estimated from EDX for these nanostructures are indicated in parts b−d.

the nucleation behavior seen for CdSe (Figure 1f) resembles that seen for selenium (Figure 1e), and δ in both cases is high enough (>10 μm^{-1}) to permit the formation of CdSe nanowires. As in previous work, we observe that the nucleation density is inversely correlated with the kinetic facility of the electrodeposition reaction: δ is low in the case of cadmium electrodeposition, a reversible and kinetically facile process, whereas δ is much higher for selenium, a kinetically hindered and electrochemically irreversible process. However, the similarity of the electrodeposits seen in Figure 1e,f leads to the hypothesis that reaction 4 is catalyzed by Se that is deposited in advance of CdSe.

This hypothesis is readily tested using a second experiment in which the nanowires produced by scanning repeatedly to negative limits of −0.60 V (Figure 2a), −0.80 V (2b), and −1.0 V (2c) are examined by SEM and EDX elemental analysis. In contrast to the experiment of Figure 1c−f, in which just one scan terminating at −0.9 V was performed, in this second experiment three voltammetric scans were performed beginning and ending at +0.60 V. Because just cadmium metal is stripped at potentials negative of +0.60 V, these scans had the effect of integrating all the CdSe and

(28) Skyllas-Kazacos, M.; Miller, B. *J. Electrochem. Soc.* **1980**, *127*, 869.
(29) Pourbaix, M. *Atlas of Electrochemical Equilibria in Aqueous Solutions*; Cebelcor: Brussels, 1974.
(30) Mishra, K. K.; Rajeshwar, K. *J. Electroanal. Chem.* **1989**, *273*, 169.

Se electrodeposited during three scans so that it could be observed and analyzed using EDX. As shown in Figure 2a, nanowires composed exclusively of selenium are produced by repetitive scans to −0.60 V. As the potential limit is extended to −0.8 V (Figure 2b), a second material that appears distinctly brighter in the SEM image is formed on top of each selenium nanowire and, concurrently, the presence of cadmium is detected in addition to selenium in the EDX analysis (Se:Cd = 2.4). Because elemental cadmium has been stripped from these nanowires, it is probable that the bright material seen in these images is CdSe. This result supports the conclusion that elemental selenium, which is deposited at step edges with high δ in advance of CdSe, reduces the barrier for the nucleation of CdSe that precedes the formation of CdSe nanowires.

If the negative limit is extended further, to −1.0 V, more CdSe is produced on each scan, together with elemental cadmium, but this excess cadmium is stripped from the deposit leaving only the CdSe. As seen in Figure 2c, CdSe now blankets the selenium nanowire produced at more positive potentials, and it is no longer visible in SEM images of these nanowires. Consistent with this interpretation is the lower Se:Cd ratio of 1.9 (Figure 2c). Much of the excess selenium present in the CdSe nanowires shown in Figure 2b can be selectively removed by thermal annealing because Se (T_m = 221 °C) and SeO_2 (T_s = 315 °C) are both much more volatile than CdSe (T_m = 1350 °C). When this annealing is carried out at 300 °C for 30 min, the image and EDX analysis data shown in Figure 2d were obtained. The Se:Cd atomic ratio of 1.1 indicates that excess selenium has been selectively removed.

III.B. CdSe Nanowire Electrodeposition Mechanism. The stoichiometry of as-deposited CdSe nanowires can be improved using an in situ electrochemical approach in which excesses of the constituent elements Se and Cd deposited on a negative voltammetric scan are anodically removed from the electrodeposit containing the desired compound during an ensuing positive scan. This cyclic electrodeposition/stripping strategy has been employed previously to obtain stoichiometric CdSe by Sailor et al.[21] and others.[16,28] We sought to adapt the Sailor method to the electrodeposition of CdSe nanowires, but our implementation of that procedure, which involves rapid (10 V s^{-1}) scanning between +0.8 V and −0.4 V, always produced selenium-rich CdSe deposits at HOPG electrode surfaces. On the titanium and nickel working electrodes employed in the Sailor study, these potential limits permitted the electrodeposition of a cadmium-rich CdSe layer (at the −0.4 V limit) and the subsequent removal from this deposit of excess cadmium. All of the electrodeposited selenium was converted into CdSe.[21]

To adapt it to the growth CdSe nanowires, we modified the Sailor procedure as follows: First, the scan rate was reduced to 20 mV s^{-1} because step edge localized nucleation was optimized at this scan rate, and second, both the positive and the negative potential limits for synthesis scans were extended. The negative potential limit was moved from −0.4 V to −1.0 V. Extension of the negative limit was required because the overpotential for CdSe electrodeposition on HOPG is greater than at metal electrodes.

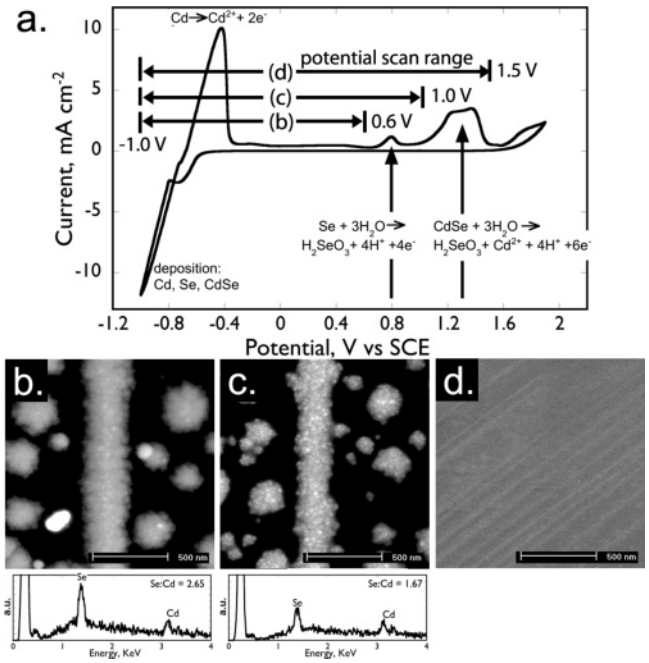

Figure 3. (a) Survey CV of a 120 mM $CdSO_4$/1 mM SeO_2 solution at pH = 2.70. (b) SEM image of HOPG electrode after first scanning to −1 V and then scanning back to 0.6 V for three cycles (inset: EDX spectrum). (c) SEM image of HOPG electrode after first scanning to −1 V and then scanning back to 1 V for three cycles (inset: EDX spectrum). (d) SEM image of HOPG electrode after first scanning to −1 V and then scanning back to 1.5 V for three cycles.

As shown in Figure 3, the extension of the positive limit permitted selenium stripping, in addition to the cadmium stripping, to occur on each positive-going scan. Shown in Figure 3a is a CV acquired in an aqueous solution containing 120 mM $CdSO_4$ and 1 mM SeO_2. Three significant oxidations occur within this voltage range: The first oxidation peak at −0.42 V is readily assigned to Cd stripping (reaction 1 in reverse).[30] To identify the other two oxidation peaks, the potential was first scanned from the rest potential to −1.0 V to deposit CdSe together with excess elemental Cd and/or Se, and then the potential was scanned positively and terminated at 0.6, 1.0, and 1.5 V. The resulting electrodeposit was characterized by SEM and EDX elemental analysis, and these data are presented in Figure 3b−d. When the potential was scanned back to 0.6 V, only cadmium oxidation occurred, and EDX shows that the nanowires are Se-rich, with a Se:Cd ratio of 2.5−3:1. When the potential was scanned to 1.0 V, SEM images (Figure 3c) show a similar nanowire morphology but a significantly smaller Se:Cd ratio of 1.5−1.7. On the basis of this observation, the second oxidation peak at +0.8 V can be assigned to the oxidation of excess selenium within the nanowires and nanoparticles to H_2SeO_3:

$$Se + 3H_2O \rightarrow H_2SeO_3 + 4H^+ + 4e^- \quad (5)$$

The chemical state of the selenium within the nanowire is assumed here to be elemental selenium because selenium oxide is soluble in this solution, but it is also possible that some SeO_2 is present and inaccessible to solution within the CdSe matrix.

If the positive limit is increased still further to +1.5 V thereby including the third oxidation peak at +1.3 V, both

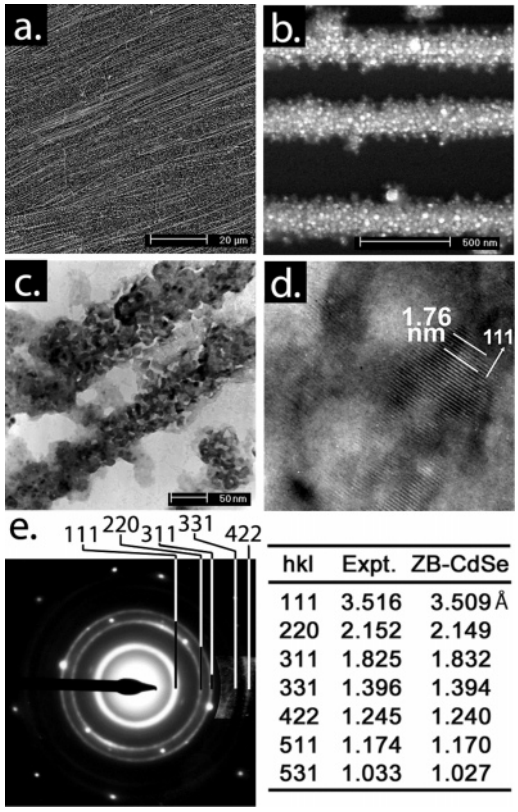

hkl	Expt.	ZB-CdSe
111	3.516	3.509 Å
220	2.152	2.149
311	1.825	1.832
331	1.396	1.394
422	1.245	1.240
511	1.174	1.170
531	1.033	1.027

Figure 4. (a) Low magnification SEM image of CdSe nanowires prepared by cycling the potential between 1 and −1 V at 20 mV s^{-1} for three cycles. (b) A higher magnification SEM image of CdSe nanowires. (c) TEM image of two CdSe nanowires prepared using the conditions indicated in part a. (d) Lattice-resolved TEM image of a CdSe nanowire showing 3.516 Å periodicity along [111] (white lines bracket five such spacings). (e) SAED pattern of CdSe nanowires. (f) Table of the experimental and literature values for zinc blende CdSe crystal.

nanoparticles and nanowires are removed from the HOPG surface (Figure 3d). We, therefore, assign this third oxidation process to CdSe stripping (the inverse of reaction 4). Thus, a positive limit of 1.0 V was employed for all subsequent CdSe nanowire synthesis experiments. The procedure for CdSe nanowire deposition was as follows: the potential was first scanned from the rest potential to −1.0 V and then scanned back to 1.0 V to strip away elemental Cd and some Se. This procedure remains imperfect because, as indicated in Figure 3c, a somewhat selenium-rich CdSe nanowire is produced. We believe this excess selenium is embedded within the CdSe matrix, is inaccessible to the electrolyte, and therefore, is not removed by reaction 5. This residual Se could be removed by annealing nanowires in N_2 at 300 °C for 30 min, as indicated in Figure 2d.

SEM and TEM characterization of the CdSe nanowires obtained using this cyclic electrodeposition/stripping scheme is presented in Figure 4. Low magnification SEM images such as that shown in Figure 4a confirm that CdSe nanowires are produced over large regions of the HOPG surface, and many of these nanowires are over 100 μm in length. Higher magnification SEM images (Figure 4b) reveal that CdSe nanowires are composed of many closely packed CdSe nanocrystallites. TEM analysis (Figure 4c) shows that these nanocrystallites have diameters ranging from 7 to 25 nm. Figure 4d shows a lattice resolved TEM image, with a plane spacing of 3.52 Å, consistent with the (111) plane spacing of cubic CdSe. The selected area diffraction pattern (SAED) of these nanowires produced sharp polycrystalline diffraction rings (Figure 4e) that are indexed to cubic CdSe (JCPDS 88-2346) as indicated in Figure 4e. The presence of elemental selenium is not directly observable in these TEM or SAED data, but it is assumed that amorphous selenium is nevertheless present in the electron amorphous regions seen in Figure 4d.

Mechanisms for the electrodeposition of CdSe have been proposed previously by Skyllas-Kazakos and Miller[29] and Mishra and Rajeshwar,[30] but these mechanisms are specific to the synthesis protocol, solution composition, and nature of the working electrode, none of which are identical to the conditions we have employed here. The sequence of reactions occurring on each electrodeposition−stripping cycle comprises the mechanism for CdSe nanowires that applies here:

Step 1 (−0.45 to −0.65 V). Reduction of H_2SeO_3 to Se proceeds via reactions 2 and 3 within the potential range from −0.45 V to −0.65 V. This selenium nucleates with a high δ of 30 μm^{-1}. Because of the high nucleation density of Se on HOPG, as demonstrated in Figure 1e, pseudo-continuous Se nanowires are formed on HOPG step edges.

Step 2 (−0.60 to −0.80 V). CdSe nanowires are formed preferentially at the electrodeposited selenium by reaction 4.

Step 3 (−0.76 to −1.00 V). Excess cadmium metal is electrodeposited according to reaction 1.

Step 4 (−1.0 to +0.60 V). Excess cadmium is stripped.

Step 5 (+0.60 to +0.80 V). Excess selenium is stripped.

III.C. Adjusting the Diameter of CdSe Nanowires. The diameter of the CdSe nanowires can be precisely controlled because it increases smoothly and gradually with the number of voltammetric cycles, *n*, as shown in Figure 5. The CV for CdSe nanowire electrodeposition is shown in Figure 5a for $n = 1$, 2, 5, and 10 cycles. It is apparent here that the prominent features of the CV remain the same as the diameter of the nanowires increase. The diameter of the CdSe nanowires spans a range from 30 nm ($n = 1$) to 300 nm ($n = 15$). The populations of nanowires produced in a particular synthesis experiment are narrowly distributed in diameter, with a relative standard deviation of the diameter that ranged from 13 to 22%. However, it should be noted that CdSe nanoparticles also nucleate on the terraces between step edges, and the number and mean diameter of these particles also increases with each voltammetric scan.

III.D. Capping CdSe Nanowires with CdS. The band gap of CdS is 2.42 eV while that of CdSe is 1.74 eV,[31] but these materials share the zinc blende crystal structure and possess similar lattice constants of 5.83 Å (CdS) versus 6.05 Å (CdSe). This structural similarity implies that CdS/CdSe interfaces with few structural defects and relatively little strain can be prepared. Moreover, the band alignments between these two materials are type 1 (nested),[32,33] favoring the localization and radiative recombination of photogenerated electrons and holes in the smaller band gap material,

(31) Chizhikov, D. M.; Shchastlivyi, V. P. *Selenium and selenides*; Collet's, Ltd.: London, 1968.
(32) Kim, B. S.; Islam, M. A.; Brus, L. E.; Herman, I. P. *J. Appl. Phys.* **2001**, *89*, 8127.
(33) Milliron, D. J.; Hughes, S. M.; Cui, Y.; Manna, L.; Li, J. B.; Wang, L. W.; Alivisatos, A. P. *Nature* **2004**, *430*, 190.

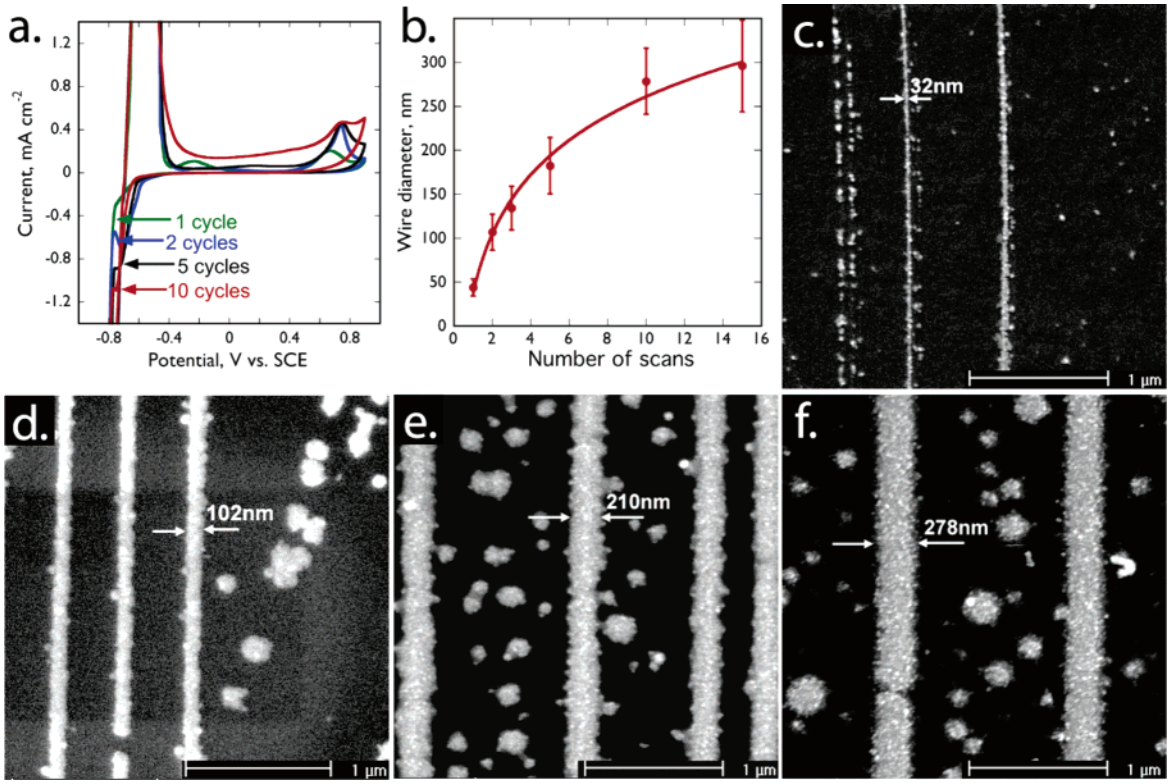

Figure 5. (a) CVs at 20 mV s^{-1} between −1.0 and 0.8 V in aqueous 100 mM $CdSO_4$ and 1 mM SeO_2 aqueous solution, pH = 2.7. (b) Plot of the CdSe nanowire diameter measured by SEM as a function of the number of deposition/stripping cycles. (c−f) SEM images of CdSe nanowires prepared using 1 (c), 2 (d), 5 (e), and 10 (f) electrodeposition/stripping cycles.

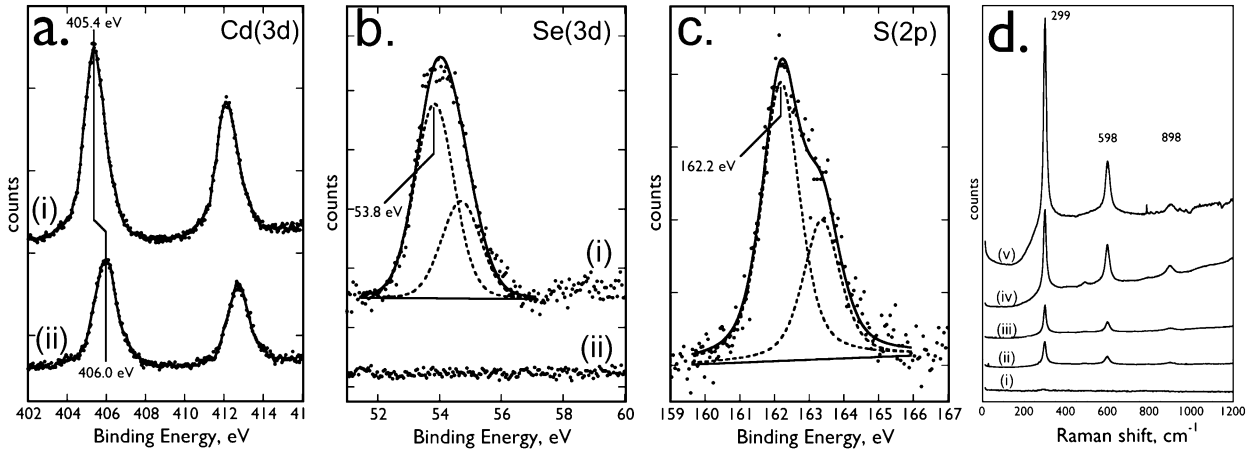

Figure 6. (a, b) XPS spectra for as-synthesized CdSe nanowires (spectrum i) and CdSe nanowires that were heated in flowing H_2S at 300 °C for 30 min (spectrum ii). (b) The experimentally observed Se(3d) emission seen in spectrum i is an envelope containing both $3d_{5/2}$ and $3d_{3/2}$ emission lines. A Gaussian deconvolution (dashed lines) shows the position of these two lines. (c) S(2p) XPS spectrum for CdSe nanowires after heating in flowing H_2S at 300 °C for 30 min. The experimentally observed emission is an envelope containing both $2p_{3/2}$ and $2p_{1/2}$ emission lines. A Gaussian deconvolution (dashed lines) shows the position of these two lines. (d) Resonance Raman spectra for CdSe nanowires after exposure to H_2S at various temperatures and for various durations: (i) 300 °C for 10 min, (ii) 60 min, and (iii) 150 min H_2S exposure and (iv) 400 °C for 30 min and (v) 1 h H_2S exposure. The transition at 299 cm^{-1} is assigned to ν_{LO}, the longitudinal optical phonon mode for CdS, and those at 598 cm^{-1} and 898 cm^{-1} are the first two overtones of this transition.[37]

CdSe, thereby eliminating or reducing recombination at surface trap states. Prior work involving layered CdSe-CdS core-shell nanoparticles[14,32] has demonstrated that these structures are capable of producing significant increases in the quantum yield for PL.

We attempted to produce a shell of CdS on top of the CdSe nanowires by replacement of Se with S during the exposure of CdSe wires to H_2S at elevated temperatures of 300 or 400 °C:

$$CdSe + H_2S \rightarrow CdS + H_2Se \qquad (6)$$

The extent to which this replacement reaction occurred could not be discerned using direct structural probes such as TEM and SAED. However, XPS and Raman spectroscopic studies show conclusively that a CdS layer is produced. These data are presented in Figure 6. Shown in Figure 6a,b are XPS spectra for as-synthesized CdSe nanowires (spectrum i) and CdSe nanowires that were exposed to H_2S at 300 °C for 30 min (spectrum ii). The sulfur region of the XPS spectrum for the CdS capped nanowires is shown in Figure 6c. A summary of the measured binding energies (Table 1) compares our observed binding energies for CdSe (for the

Table 1. Summary of XPS Analyses for CdSe and CdS-Capped CdSe Nanowires

Cd($3d_{5/2}$)		Se($3d_{5/2}$)		S($2p_{3/2}$)	
sample	BE (eV)	sample	BE (eV)	sample	BE (eV)
as-deposited CdSe	405.4	as-deposited CdSe	53.8	as-deposited CdSe	not observed
CdSe/CdS	406.0	CdSe/CdS	not observed	CdSe/CdS	162.2
		Literature Values[a]			
elemental Cd	404.9−405.1[40−42]	elemental Se	55.5[24]	elemental S	164.1[24]
$Cd(OH)_2$	404.8−405.1[24,41]				
CdO	404.2[40]				
CdSe	405.3[40]	CdSe	54.0−54.7[43,44]		
CdS	405.2−405.4[40,45,46]			CdS	161.4−161.8[45]
		SeO_2	59.9		
$CdSO_4$	405.4[46]			$CdSO_4$	168.8[46]

[a] Reference data courtesy of NIST Photoelectron Spectroscopy Database (http://srdata.nist.gov/xps/) and ref 24.

as-synthesized nanowires) and CdS-capped CdSe (for the nanowires exposed to H_2S) and the binding energies of alterative candidate compounds that might be present on these surfaces. The XPS analysis of the as-synthesized CdSe nanowires yields binding energies of 405.4 eV for the Cd($3d_{5/2}$) binding energy and 53.8 eV for the Se($3d_{5/2}$) binding energy (Table 1), and these values are both consistent with the expected chemical shifts for CdSe. For CdS-capped CdSe nanowires, however, our measured binding energies for Cd($3d_{5/2}$) and S($2p_{3/2}$) are both shifted to higher binding energy by approximately 0.6 eV from what would be expected for a bulk CdS sample. We have used the C(1s) peak of the HOPG substrate at 284.5 eV as the energy scale reference for all the spectra presented here. One explanation for this 0.6 eV shift is that it is an offset caused by a junction potential associated with the conduction band edge offset between the CdS surface layer and the CdSe inner core,[33] which is in direct contact with the graphite substrate.

The thickness of the CdS layer formed on the CdSe nanowires cannot be determined from these data. However, as seen by comparing parts a and b of Figure 5, the CdS layer is sufficiently thick to completely attenuate the signal from the underlying Se($3d_{5/2}$). This does allow us to put a lower limit on the thickness of the CdS capping layer. The kinetic energy of the Se($3d_{5/2}$) photoelectrons is 1199.8 eV. For the capped nanowires the Se($3d_{5/2}$) photoelectrons are inelastically scattered as they transit the CdS capping layer. The inelastic mean free path for electrons of this kinetic energy in CdS is expected to be 2.7 nm.[34] The signal-to-noise ratio for the Se($3d_{5/2}$) peak from the as-prepared CdSe nanowire sample is ~20 (Figure 6b, i). To attenuate the Se($3d_{5/2}$) photoelectron signal by a factor of 20, the CdS capping layer on these ≈150 nm diameter (CdSe + CdS) wires would have to be at least 8.1 nm thick. The thickness of the CdS layer is expected to be a function both of the exposure duration to H_2S and of the temperature.

As-synthesized CdSe nanowires did not produce observable Raman scattering using 514.5 nm light (2.4 eV), and this is likely because this excitation energy is well off-resonance for the 1.74 eV CdSe band edge.[35,36] In contrast, resonantly enhanced Raman scattering peaks for CdS (band gap = 2.42 eV) emerged as CdSe nanowires were heated in

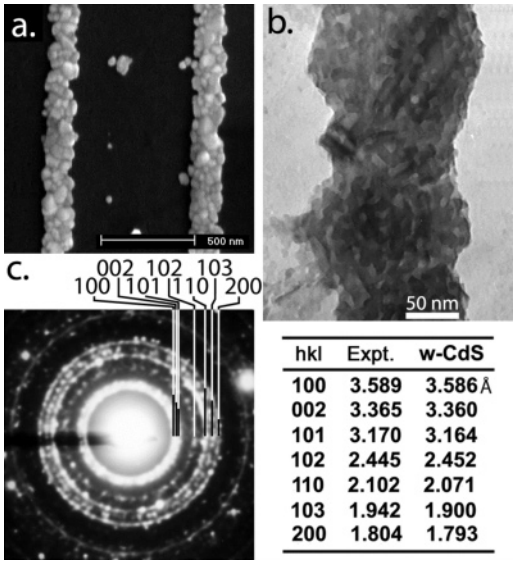

Figure 7. SEM image (a), TEM image (b), and SAED pattern (c) for CdSe nanowires after annealing in H_2S at 400 °C for 1 h.

H_2S (Figure 6d). The most prominent transition at 299 cm^{-1} is assigned to ν_{LO}, the longitudinal optical phonon mode for CdS, and two overtones of this transition at 598 cm^{-1} and 898 cm^{-1} were also observed.[37] The intensity of these peaks correlated with the exposure time at 300 °C (Figure 6d, spectra i−iii) and become even more intense for exposures that were carried out at 400 °C (spectra iv and v). ν_{LO} for CdS is shifted higher in energy from the corresponding transition at CdSe ($\nu_{LO} \approx 200$ cm^{-1}),[37] and it is, therefore, clear that the surface of CdSe nanowires is converted into CdS with exposure to H_2S at either 300 or 400 °C.

Heat treatment in flowing H_2S at 400 °C for 1 h or more caused CdSe nanowires to be converted completely into CdS. This conversion process did not alter the morphology of these nanowires (Figure 7a,b), but SAED spectra of such wires could be indexed to hexagonal CdS, as shown in Figure 7c. As already indicated, these nanowires also produced intense resonance Raman scattering at energies characteristic of CdS (Figure 6d, spectrum v).

III.E. PL Spectroscopy of CdSe and CdSe-CdS Core-Shell Nanowires. PL spectroscopy was used to characterize electrodeposited nanowires and nanoparticles. Nanoparticle emission could not be excluded from these spectra because of the proximity of these particles to nanowires on the HOPG

(34) Powell, C. J.; Jabolonski, A. NIST Electron Mean Free Path Database, Version 1.1.
(35) Leite, R. C. C.; Porto, S. P. S. *Phys. Rev. Lett.* **1966**, *17*, 10.
(36) Scott, J. F.; Leite, R. C. C.; Damen, T. C. *Phys. Rev.* **1969**, *188*, 1285.
(37) Zou, S. Z.; Weaver, M. J. *J. Phys. Chem. B* **1999**, *103*, 2323.

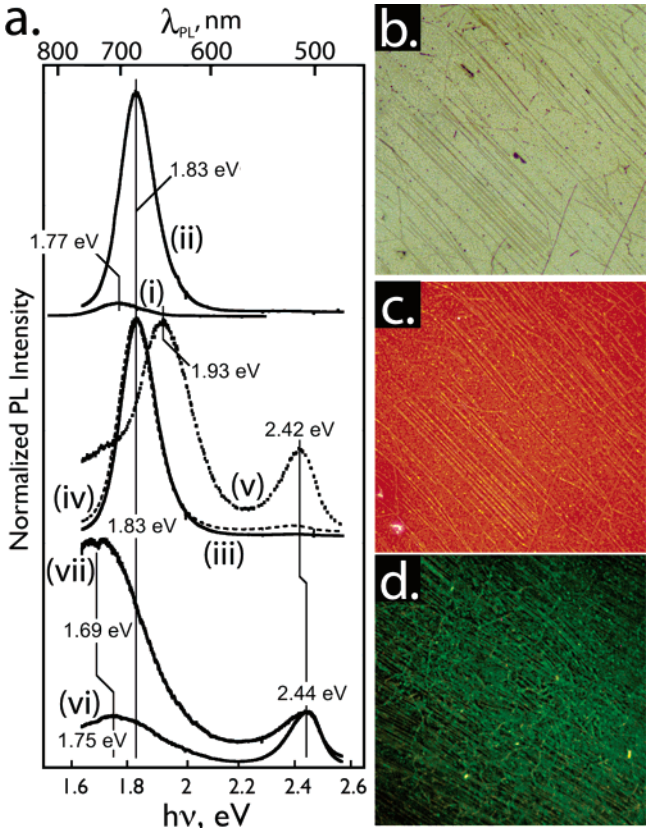

Figure 8. (a) PL spectra for CdSe and CdS-capped CdSe nanowires as follows: (i) As-synthesized CdSe nanowires after annealing in N_2 for 30 min. (ii) As-synthesized CdSe nanowires after heating in H_2S at 300 °C for 1 h; (iii−v) as-synthesized CdSe nanowires after annealing in H_2S at 300 °C for 1 h (iii), 3 h (iv), and 10 h (v; the peak intensity was normalized to the maximum intensity for each spectrum); and (vi, vii) CdSe nanowires after annealing in H_2S at 400 °C for 1 h (vi) and 4 h (vii), respectively (the peak intensity is normalized at 2.45 eV). (b) Photomicrograph of CdSe nanowires after annealing in H_2S at 300 °C for 1 h acquired using white-light, bright-field illumination, (c) the same nanowires as in part b with oblique illumination at 257 nm, and (d) photomicrograph of CdS nanowires prepared by exposure of as-synthesized CdSe nanowires to H_2S at 400 °C for 60 min seen with oblique illumination at 257 nm.

surface and the fact that emission was acquired from a 300 μm diameter area of the surface. Typical PL spectra are shown in Figure 8a. PL emission from as-synthesized CdSe nanowires was weak (data not shown), but band edge emission characteristic of CdSe at 1.77 eV was detectable for nanowires that were annealed in N_2 at 300 °C for 30 min (Figure 8a, spectrum i). As indicated in Figure 2d, the effect of this heat treatment is to eliminate excess selenium from the as-deposited CdSe nanowires, thereby rendering them very nearly stoichiometric. These CdSe nanowires were then exposed to H_2S at 300 °C for 60 min. and spectrum ii was acquired. The increase in intensity seen here is approximately 15-fold, and a slight (6 meV) blue shift of the emission is also observed. The increased PL intensity observed here is similar to that reported previously by Manna et al.[23] who investigated the effect of CdS and ZnS capping of CdSe nanocrystals; however, the spectral shift is in the opposite direction as seen in that work. The reason for this difference can be rationalized as follows: The red-shifted PL emission seen by Manna et al. is caused by an increase in the nanocrystal volume accessible to photogenerated electrons resulting from the fact that electrons in the conduction band of CdSe are partially delocalized in the CdS shell because the band offset at the CdSe/CdS interface is just ≈0.2 eV.[23] The PL emission for the CdS-capped CdSe nanowires that are probed here shows no quantum confinement so the addition of a CdS shell would not be expected to cause a red shift of the emission. The origin of the slight blue shift induced by that seen here cannot be definitively determined from our data, but one possibility is the elimination by the CdS capping layer of surface trap states that are contributing red-shifted emission to the spectra of CdSe nanowires seen in Figure 8a. CdS-capped CdSe nanowires are shown in the optical micrographs of Figure 8b,c that were acquired using bright field illumination and 257 nm excitation, respectively. A careful comparison of these images confirms that light emission is indeed from the nanowires, and the light intensity distribution along the axis of individual nanowires is uniform.

Spectra iii−v document the effect of H_2S (300 °C) exposure time on the PL spectrum. These exposures were 1, 3, and 10 h, respectively. Longer exposures to 300 °C H_2S of 3 h and 10 h are associated with the emergence of a new emission peak at 2.41 eV that is assigned to the CdS band edge emission. After 3 h, CdS emission accounts for 8% of the emitted photons, and this fraction increases to 42% after 10 h. This progression of spectra i−v is the logical consequence of two processes, the first involving the formation of a CdS shell of increasing thickness at the surface of the CdSe nanowire and the second involving the formation of an increasing S-rich terniary core, $CdSe_xS_{1-x}$. This second process is assumed to be responsible for the observed blue shift seen for the "CdSe band edge" emission from spectra iv and v from 1.83 to 1.93 eV. When the annealing time is 1 h or less, the CdS layer that is produced is thin relative to the diffusion length of photoexcited carriers, and these carriers are able to efficiently thermalize into the CdSe core prior to recombination. Longer exposures produce a thicker CdS layer that exceeds the diffusion length of carriers, and some radiative recombination within this CdS shell is, therefore, observed. The prominence of CdS shell emission increases with exposure time and the thickness of the CdS shell.

Not surprisingly, increasing the temperature of the furnace to 400 °C accelerates the process of CdS shell formation in H_2S. Spectra vi and vii in Figure 8a show the emission spectra of CdSe nanowires after exposures of 1 and 3 h, respectively. Now, a CdS band edge emission peak at 2.44 eV is observed after just 1 h of exposure to H_2S (spectrum vi). As shown in the optical micrograph of Figure 8d, these nanowires appear green in color. It is tempting to assign the remaining peak, at 1.60−1.75 eV, to CdSe band-edge emission, but electron diffraction analysis of these nanowires (Figure 7c) provides no evidence for unreacted CdSe. Consequently, it is likely, but not certain, that this "CdSe" emission is the well-known[38,39] trap-state emission associated

(38) Berndt, R.; Gimzewski, J. K. *Phys. Rev. B* **1992**, *45*, 14095.
(39) Shiraki, Y.; Shimada, T.; Komatsub, K. *J. Appl. Phys.* **1974**, *45*, 3554.
(40) Gaarenstroom, S. W.; Winograd, N. *J. Chem. Phys.* **1977**, *67*, 3500.
(41) Hammond, J. S.; Gaarenstroom, S. W.; Winograd, N. *Anal. Chem.* **1975**, *47*, 2194.
(42) Nyholm, R.; Martensson, N. *Solid State Commun.* **1981**, *40*, 311.

with Cd^{2+} vacancies in CdS. This assignment provides an explanation for the increased intensity (relative to the 2.44 eV band edge peak) of the 1.75 eV band as a function of H_2S annealing time.

IV. Conclusions

We describe a new synthesis of CdSe nanowires and CdSe-CdS core-shell nanowires by cyclic electrodeposition/stripping coupled with step edge decoration on HOPG surfaces. The data presented here support the following conclusions:

1. CdSe nanowires that are nearly stoichiometric are produced using the cyclic electrodeposition/stripping method in concert with thermal annealing in N_2 to eliminate selenium.

2. The nanowire length can exceed 100 μm, and these nanowires are organized into parallel arrays on the HOPG surface, mimicking the organization of step edges present on these surfaces.

3. The synthesis of CdSe nanowires with diameters as small as 30 nm is made possible by an unsual nucleation mechanism in which selenium nuclei, depositing at potentials positive of CdSe, are formed with a high linear density ($\delta > 30\ \mu m^{-1}$) on step edge defects. The subsequent electrodeposition of CdSe occurs preferentially atop these nuclei. CdSe nanowires of larger diameters, up to 300 nm, can be selectively obtained by increasing the number of electrodeposition−stripping cycles that are applied.

4. TEM and SAED results show that the CdSe nanowires are composed of many zinc blende CdSe nanocrystallites.

5. CdSe nanowires exhibit band edge PL emission at 1.74 eV, with no defect emission observed. When the polycrystalline nature of these nanowires is considered, the absence of the observable trap state emission is surprising and significant. The quantum efficiency of this emission is increased by a factor of 15 with the addition of a CdS shell.

Acknowledgment. This work was funded by the National Science Foundation (Grant DMR-0405477) and by the Petroleum Research Fund administered by the American Chemical Society (Grant 40714-AC5). Q.L. gratefully acknowledges an American Chemical Society, Division of Analytical Chemistry, Graduate Summer Fellowship, sponsored by Johnson & Johnson Pharmaceutical Research & Development, L.L.C. J.C.H. acknowledges funding support from the Department of Energy (Grant DE-FG03-96ER45576). Graphite for this work was supplied by a grant from the EU Commission FP6 NMP-3 Project No. 505457-1 ULTRA-1D.

CM060262L

(43) Polak, M. *J. Electron. Spectrosc. Relat. Phenom.* **1982**, *28*, 171.
(44) Shenasa, M.; Sainkar, S.; Lichtman, D. *J. Electron. Spectrosc. Relat. Phenom.* **1986**, *40*, 329.
(45) Marychurch, M.; Morris, G. C. *Surf. Sci.* **1985**, *154*, L251.
(46) Riga, J.; Verbist, J. J.; Josseaux, P.; Mesmaeker, A. K. *Surf. Interface Anal.* **1985**, *7*, 163.
(47)